

# ChemComm

Accepted Manuscript



This is an *Accepted Manuscript*, which has been through the Royal Society of Chemistry peer review process and has been accepted for publication.

*Accepted Manuscripts* are published online shortly after acceptance, before technical editing, formatting and proof reading. Using this free service, authors can make their results available to the community, in citable form, before we publish the edited article. We will replace this *Accepted Manuscript* with the edited and formatted *Advance Article* as soon as it is available.

You can find more information about *Accepted Manuscripts* in the [Information for Authors](#).

Please note that technical editing may introduce minor changes to the text and/or graphics, which may alter content. The journal's standard [Terms & Conditions](#) and the [Ethical guidelines](#) still apply. In no event shall the Royal Society of Chemistry be held responsible for any errors or omissions in this *Accepted Manuscript* or any consequences arising from the use of any information it contains.

Cite this: DOI: 10.1039/c0xx00000x

www.rsc.org/xxxxxx

ARTICLE TYPE

## Electrochemical investigation of sodium reactivity with nanostructured Co<sub>3</sub>O<sub>4</sub> for sodium-ion batteries

Md Mokhlesur Rahman\*, Alexey M. Glushenkov, Thrinathreddy Ramireddy, Ying Chen

Received (in XXX, XXX) Xth XXXXXXXXX 20XX, Accepted Xth XXXXXXXXX 20XX

DOI: 10.1039/b000000x

The electrochemical behaviour of Co<sub>3</sub>O<sub>4</sub> with sodium is reported here. Upon cycling in the voltage window of 0.01-3.0V, Co<sub>3</sub>O<sub>4</sub> undergoes conversion reaction and exhibits a reversible capacity of 447 mAh g<sup>-1</sup> after 50 cycles. Therefore, nanostructured Co<sub>3</sub>O<sub>4</sub> presents feasible electrochemical sodium storage, offering possibilities to develop new anode materials for sodium-ion batteries.

Current interest in Na-ion based batteries arises from the potential of these devices to become less expensive, safer and environmentally benign with respect to present Li-ion technologies. In a world with a growing concern about energy management issues, sodium has strongly broken into energy storage research field. This alkali holds promise for being a complement or substituting Li-based technology.<sup>1</sup> Its natural abundance, easy access to sodium sources and, consequently, lower price; suitable redox potential (-2.71 V, vs. standard hydrogen electrode) and similar intercalation chemistry to Li, make this element strategic in innovative research of energy storage systems.<sup>1-3</sup> However, the radius of sodium ions (1.06 Å) is obviously larger than that of lithium ions (0.76 Å), which makes it more difficult to identify electrode materials for Na-ion batteries.<sup>4</sup> Therefore, in order to make sodium-ion batteries viable, identification of suitable anode and cathode materials is critical. Even though, a variety of sodium host cathodes have been reported to have certain Na-storage capacity and cycleability,<sup>5-9</sup> but the anodic host have been less successfully developed.

Just as lithium counterparts, the anode materials for sodium-ion batteries are expected to operate via a range of similar mechanisms, e.g. intercalation, alloying-dealloying and conversion reactions. It has been demonstrated, however, that many materials considered as promising anode materials for lithium-ion batteries do not work at all or demonstrate only a limited redox electrochemical activity in sodium-ion batteries. For example, graphite, the most used commercial anode material in lithium-ion batteries can intercalate virtually no sodium and, consequently, is not a prospective anode for sodium-ion batteries.<sup>3</sup> Two other popular large capacity anode materials for lithium-ion batteries, silicon and germanium, have no detectable redox electrochemical activity in sodium-ion batteries.<sup>10</sup> Some other materials, e.g. hard carbons, are electrochemically active in Na-ion batteries while their reactivity with lithium is very

limited.<sup>3,11-13</sup> On the contrary, many metal oxides are well known for lithium storage but still remain unexplored for analogous sodium storage.

Until now, only a few studies have reported the sodium storage properties of metal oxides, including Fe<sub>3</sub>O<sub>4</sub> and α-Fe<sub>2</sub>O<sub>3</sub>,<sup>14</sup> Sb<sub>2</sub>O<sub>4</sub> thin film,<sup>15</sup> TiO<sub>2</sub> nanotubes,<sup>16</sup> NiCo<sub>2</sub>O<sub>4</sub>,<sup>17</sup> α-MoO<sub>3</sub>,<sup>18</sup> and SnO<sub>2</sub>.<sup>19</sup> These works provide some information on sodium electrochemistry of metal oxides and their possibility to use as anodes for the development of sodium-ion batteries. Here we attempted to extend the electrochemical investigation of cobalt oxide (Co<sub>3</sub>O<sub>4</sub>) with sodium. In this study, we have demonstrated a possible conversion reaction of Co<sub>3</sub>O<sub>4</sub> with sodium with a reversible capacity of 447 mAh g<sup>-1</sup> and ~ 86 % capacity retention after 50 cycles.

The Co<sub>3</sub>O<sub>4</sub> powder was synthesized by single step molten salt precipitation process (for experimental details, see ESI). The XRD pattern of the Co<sub>3</sub>O<sub>4</sub> powder is shown in Fig. 1a. All diffraction peaks are consistent with the cubic phase of Co<sub>3</sub>O<sub>4</sub> [JCPDS no. 00-043-1003, space group *Fd-3m* (no. 227)]. No peaks of any other phases or impurities were detected, demonstrating that materials with high purity could be obtained using the present synthesis strategy. The diffraction peaks at 19.0, 31.2, 36.8, 44.8, 59.3 and 65.2° are associated with the 111, 220, 311, 400, 511, and 440 reflections of Co<sub>3</sub>O<sub>4</sub>, indicating successful synthesis of Co<sub>3</sub>O<sub>4</sub>. Fig. 1b shows SEM image of the Co<sub>3</sub>O<sub>4</sub> powder. It is found that Co<sub>3</sub>O<sub>4</sub> sample consists of agglomerated clusters of nanoparticles with a pyramid like morphology (inset of Fig1b). More SEM images are shown in Fig. S1 (ESI), which further depicts the morphological features of Co<sub>3</sub>O<sub>4</sub> sample.

To obtain information concerning structural and morphological evolution of the sample, TEM measurements were carried out. Bright-field imaging of the sample reveals dense agglomerates of fine (<10 nm) and much coarser (> 30 nm) crystalline Co<sub>3</sub>O<sub>4</sub> (Fig. 2a and Fig. S2 (ESI)). The corresponding selected area electron diffraction (SAED) pattern is depicted in Fig. 2b. The SAED pattern consists of single component of Co<sub>3</sub>O<sub>4</sub> with a *d* spacing of 0.476, 0.288, 0.242, 0.211, and 0.156 nm which can be referred to the crystallographic directions of (111), (220), (311), (400), and (511), respectively. This result is consistent with the XRD pattern obtained for this sample as shown in Fig.1a. A HRTEM image is shown in Fig. 2c. The marked *d*-spacing of 0.291 nm corresponding well with that of (220) planes of cubic Co<sub>3</sub>O<sub>4</sub>.

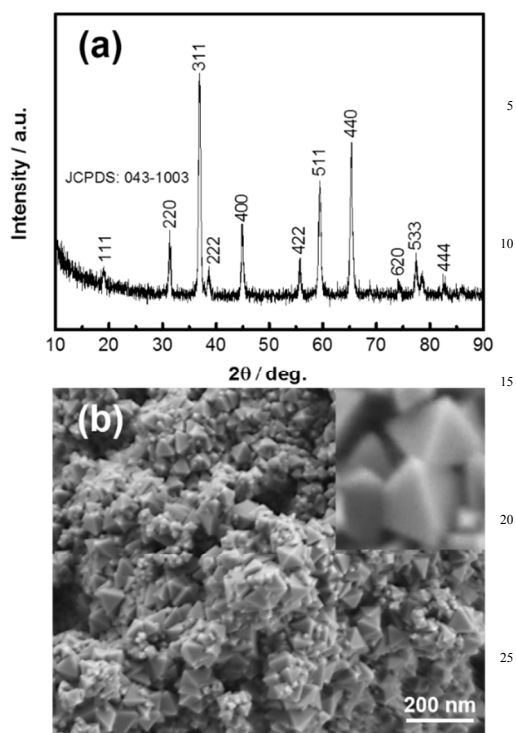


Fig. 1 (a) XRD pattern and (b) SEM image of  $\text{Co}_3\text{O}_4$  sample.

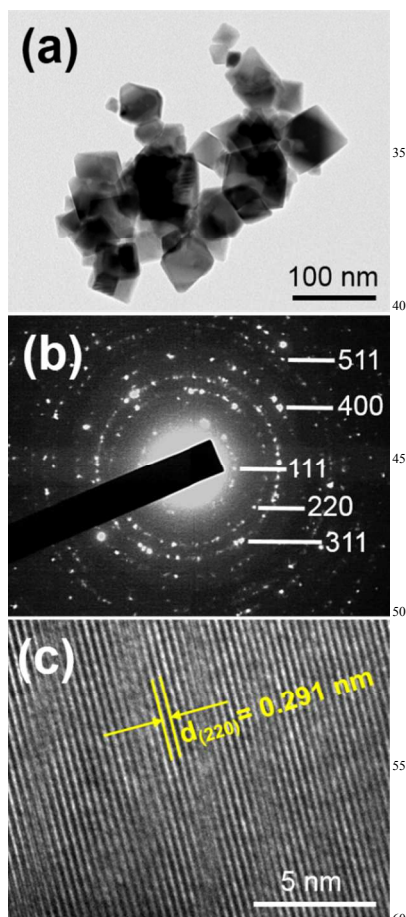
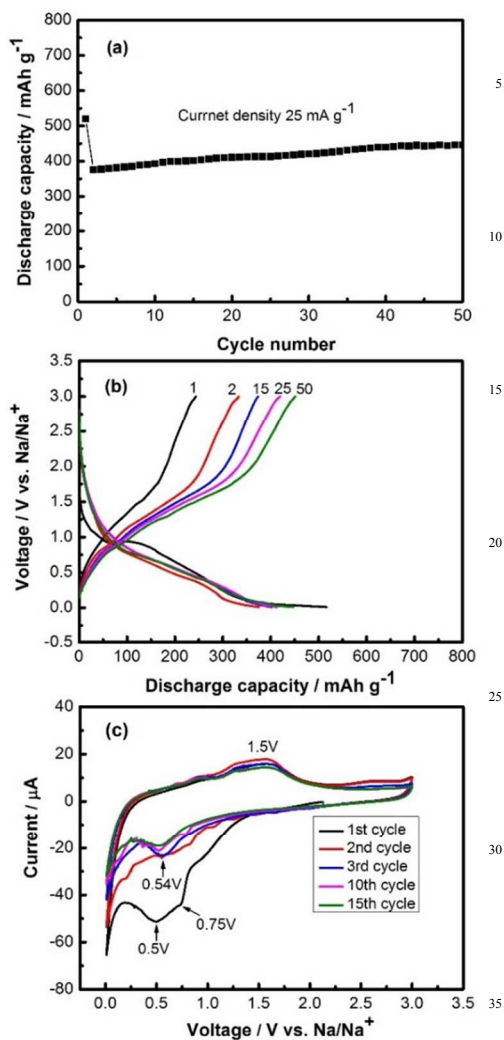
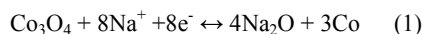


Fig. 2 TEM images of  $\text{Co}_3\text{O}_4$  sample: (a) a bright-field image; (b) corresponding SAED pattern; and (c) HRTEM image of  $\text{Co}_3\text{O}_4$  crystal with a  $d$  spacing of 0.291 nm corresponding well with that of (220) planes.

The electrochemical performance of the  $\text{Co}_3\text{O}_4$  electrodes was evaluated using CR 2032 coin-type cells in which Na metal was used as the counter/reference electrode (for experimental details, see ESI). The cells were galvanostatically discharged-charged in the voltage range of 0.01-3.0 V. Fig. 3a shows the cycling performance of  $\text{Co}_3\text{O}_4$  electrode at a current density of  $25 \text{ mA g}^{-1}$ . The measured 1<sup>st</sup> and 50<sup>th</sup> cycle discharge/charge capacities were 520/245 and 447/446  $\text{mAh g}^{-1}$  with a Coulombic efficiency of  $\sim 47\%$  for the 1<sup>st</sup> and  $\sim 100\%$  for the 50<sup>th</sup> cycle, respectively. At the 50<sup>th</sup> cycle, the  $\text{Co}_3\text{O}_4$  electrode delivered a reversible capacity of 447  $\text{mAh g}^{-1}$ , which is  $\sim 86\%$  of the initial discharge capacity. Fig. 3b presents the discharge-charge voltage profiles for the 1<sup>st</sup>, 2<sup>nd</sup>, 15<sup>th</sup>, 25<sup>th</sup>, and 50<sup>th</sup> cycle at a current density of  $25 \text{ mA g}^{-1}$ . The first discharge curve displayed all the characteristic features related to the various stages of sodiation. The first discharge profile exhibits a plateau around 0.8V (SEI layer formation) and a bump around 0.6 V, followed by a long tail at a lower voltage. The features of the first discharge curve confirm that conversion process is existing for the sodiation of  $\text{Co}_3\text{O}_4$  electrode. However, the SEI layer formation voltage of  $\text{Co}_3\text{O}_4$  electrode is different between Na-ion and Li-ion system. Na/ $\text{Na}^+$  system shows lower SEI layer formation voltage ( $\sim 0.8\text{V}$ ) than that of Li/ $\text{Li}^+$  system (above 0.8V) and SEI layer formation plateau for Na/ $\text{Na}^+$  system is not as sharp/long as Li-ion cell.<sup>20, 21</sup> On the other hand, the initial sodiation capacity of  $\text{Co}_3\text{O}_4$  electrode is much lower than Li-ion cell.<sup>20, 21</sup> Therefore, these two points are reinforcing the idea that a full conversion could not occur in this sodiation process initially. The voltage platform of the charge curves upon desodiation were quite similar to those of de-lithiation. Only difference is the process of  $\text{Na}^+$  release at a lower voltage of  $\sim 1.5\text{V}$  compared to that of  $\text{Li}^+$  ( $\sim 2.1\text{V}$ ).

To further assess the electrochemical reactivity of  $\text{Co}_3\text{O}_4$  with Na, cyclic voltammetry studies were performed at a scan rate of  $0.05 \text{ mV s}^{-1}$  in the voltage range of 0.01-3.0V (Fig. 3c). The first cycle reduction (cathodic scan) results in a broad peak centred at  $\sim 0.5\text{V}$  with a small peak at 0.75 V. This reduction process is corresponding to the partial reduction of  $\text{Co}_3\text{O}_4$  to metallic cobalt (Co), the electrochemical formation of  $\text{Na}_2\text{O}$ , and the formation of a partially irreversible solid electrolyte interphase (SEI) layer. The broad feature of this reduction peak is also consistent with the partial conversion process initially. A full conversion process gives a very strong sharp peak in the first reduction process for the Li-ion cell.<sup>22, 23</sup> In the subsequent 110 cycles, only one cathodic peak can be observed at around 0.54V. However, peaks are positively shifted to a higher voltage with respect to the first cycle, which is ascribed to the polarisation effect of the electrode in the first cycle.<sup>24</sup> In the oxidation process (anodic scan), there is a peak at 1.5V, corresponds to the re-oxidised of Co to  $\text{Co}_3\text{O}_4$  and  $\text{Na}_2\text{O}$  decomposes. Theoretically, the formation of Co and  $\text{Na}_2\text{O}$  and the re-formation of  $\text{Co}_3\text{O}_4$  can be described by the following electrochemical conversion reaction:



**Fig. 3** Electrochemical performance of  $\text{Co}_3\text{O}_4$  electrodes at 0.01–3.0 V (vs.  $\text{Na}/\text{Na}^+$ ): (a) cycling performance at a current density of  $25 \text{ mA g}^{-1}$ ; (b) corresponding galvanostatic discharge-charge voltage profiles for the 1<sup>st</sup>, 2<sup>nd</sup>, 15<sup>th</sup>, 25<sup>th</sup>, and 50<sup>th</sup> cycle; and (c) cyclic voltammogram recorded at a scan rate of  $0.05 \text{ mV s}^{-1}$  between 0.01 and 3.0V.

In order to determine the Na-storage mechanism in  $\text{Co}_3\text{O}_4$ , *ex situ* XRD measurements were performed on electrodes after cycling (Fig. 4). Fig. 4a shows *ex situ* XRD patterns of the fully discharged-charged electrodes for the first cycle. First cycle discharge to 0.01V, XRD pattern demonstrates that all diffraction peaks are well indexed to the cubic  $\text{Co}_3\text{O}_4$  phase (JCPDS no. 00-043-1003) with a small unknown peak at around  $32.7^\circ$ . First cycle charge back to 3.0V, *ex situ* XRD pattern confirms the existence of  $\text{Co}_3\text{O}_4$  phase. To get further information, we selected the 20<sup>th</sup> cycle fully discharged-charged electrode for *ex situ* XRD measurements (Fig. 4 b). Surprisingly, all diffraction peaks for the  $\text{Co}_3\text{O}_4$  phase tend to disappear and a new phase of  $\text{Na}_2\text{O}$  (JCPDS no. 00-003-1074) appears when electrode was discharged to 0.01V. At the same time there should also have evidence of Co (JCPDS no. 00-015-0806) phase formation.

Unfortunately there is significant overlap of this peak with copper current collector peak in the measured XRD patterns. On the other hand, when electrode was charged back to 3.0V, all diffraction peaks for the  $\text{Co}_3\text{O}_4$  phase appear. These findings suggest that the conversion reaction is not completed in the first discharge to 0.01V, thus the  $\text{Co}_3\text{O}_4$  phase still exists in the first discharge and visible again when charge back to 3.0V. The conversion reaction tends to take place fully with increasing cycling number. It is anticipated that discharge capacity will keep increasing until all materials get involved in the conversion reaction and then capacity will keep constant or may decline.

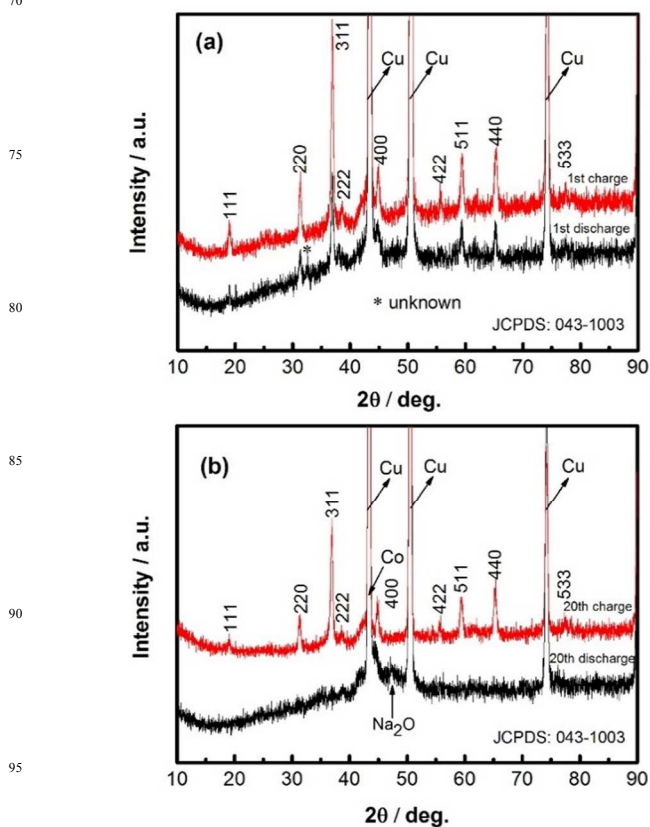


**Fig. 4** *ex-situ* XRD patterns of  $\text{Co}_3\text{O}_4$  electrodes: (a) First cycle fully discharged-charged state; (b) 20<sup>th</sup> cycle fully discharged-charged state.

In conclusion, low temperature molten salt synthesis of nanostructured  $\text{Co}_3\text{O}_4$  with a bimodal size distribution of particles, very fine ( $< 10 \text{ nm}$ ) and coarser ( $> 30 \text{ nm}$ ) has successfully been achieved. The electrochemical sodiation/de-sodiation of nanostructured  $\text{Co}_3\text{O}_4$  was reversible over an extended voltage range of 0.01–3.0 V vs.  $\text{Na}/\text{Na}^+$ . Overall, these preliminary results indicate that  $\text{Co}_3\text{O}_4$  could be used as a possible negative electrode for more sustainable cost-effective Na-ion batteries. Discharging  $\text{Co}_3\text{O}_4$  at a lower voltage of 0.01V vs.  $\text{Na}/\text{Na}^+$  offers a characteristic voltage profile for oxide conversion similar to that occurring upon lithiation of  $\text{Co}_3\text{O}_4$ , however, sodiation was not as pronounced as that caused by lithiation. This was likely due to the larger size of the  $\text{Na}^+$  ions and their reduced mobility. Charging back to 3.0V vs.  $\text{Na}/\text{Na}^+$  upon de-sodiation was quite similar to those of de-lithiation. The

reversible capacity as high as 447 mAh g<sup>-1</sup> was attained after 50 cycles at 25 mA g<sup>-1</sup> current, being this value still comparable with those of other state-of-the-art materials for Na-ion batteries. Moreover, the obtained result is undoubtedly helpful to further advance towards sodium electrochemistry of nanostructured Co<sub>3</sub>O<sub>4</sub>.

Financial support from the Australian Research Council under the Discovery Project (DP) and Deakin University Central Research Grant Scheme, 2013, is acknowledged.

## Notes and references

Institute for Frontier Materials, Deakin University, Waurn Ponds, VIC 3216, Australia.

Fax: + 61352271103; Phone: +61352272642

E-mail: m.rahman@deakin.edu.au

† Electronic Supplementary Information (ESI) available: Experimental details, SEM, and TEM. See DOI: 10.1039/b000000x/

- 1 V. Palomares, M. Casas-Cabanas, E. Castillo-Martínez, M. H. Han, T. Rojo, *Energy Environ. Sci.*, 2013, **6**, 2312.
- 2 J. Qian, Y. Chen, L. Wu, Y. Cao, X. Ai, H. Yang, *Chem. Commun.*, 2012, **48**, 7070.
- 3 S. W. Kim, D.H. Seo, X.H. Ma, C. Ceder, K. Kang, *Adv. Energy Mater.*, 2012, **2**, 710.
- 4 M. D. Slater, D. Kim, E. Lee, C. S. Johnson, *Adv. Funct. Mater.*, 2013, **23**, 947.
- 5 Y. Cao, L. Xiao, W. Wang, D. Choi, Z. Nie, J. Yu, L. V. Saraf, Z. Yang, J. Liu, *Adv. Mater.*, 2011, **23**, 3155.
- 6 R. Berthelot, D. Carlier, C. Delmas, *Nat. Mater.*, 2011, **10**, 74.
- 7 J. Qian, M. Zhou, Y. Cao, X. Ai, H. Yang, *Adv. Energy Mater.*, 2012, **2**, 410.
- 8 M. Zhou, L. Zhu, Y. Cao, R. Zhao, J. Qian, X. Ai, H. Yang, *RSC Advances*, 2012, **2**, 5495.
- 9 R. Zhao, L. Zhu, Y. Cao, X. Ai, H. X. Yang, *Electrochem. Commun.*, 2012, **21**, 36.
- 10 V. L. Chevrier, G. Ceder, *J. Electrochem. Soc.*, 2011, **158**, A1011.
- 11 V. Palomares, P. Serras, I. Villaluenga, K. B. Hueso, J. Carretero-Gonzalez, T. Rojo, *Energy Environ. Sci.*, 2012, **5**, 5884.
- 12 M.D. Slater, D. Kim, E. Lee, C.S. Johnson, *Adv. Funct. Mater.*, 2013, **23**, 947.
- 13 B.L. Ellis, L.F. Nazar, *Solid State and Materials Science*, 2012, **16**, 168.
- 14 S. Komaba, T. Mikumo, N. Yabuuchi, A. Ogata, H. Yoshida, Y. Yamada, *J. Electrochem. Soc.*, 2010, **157**, A60.
- 15 Q. Sun, Q.Q. Ren, H. Li, Z.W. Fu, *Electrochem. Commun.*, 2011, **13**, 1462.
- 16 H. Xiong, M.D. Slater, M. Balasubramanian, C.S. Johnson, T. Rajh, *J. Phys. Chem. Lett.*, 2011, **2**, 2560.
- 17 R. Alcantara, M. Jaraba, P. Lavela, J.L. Tirado, *Chem. Mater.*, 2002, **14**, 2847.
- 18 S. Hariharan, K. Saravanan, P. Balaya, *Electrochem. Commun.*, 2013, **31**, 5.
- 19 Y. Wang, D. Su, C. Wang, G. Wang, *Electrochem. Commun.*, 2013, **29**, 8.
- 20 X. Guo, W. Xu, S. Li, Y. Liu, M. Li, X. Qu, C. Mao, X. Cui, C. Chen, *Nanotechnology*, 2012, **23**, 465401.
- 21 X. Yang, K. Fan, Y. Zhu, J. Shen, X. Jiang, P. Zhao, C. Li, *J. Mater. Chem.*, 2012, **22**, 17278.
- 22 M.M. Rahman, J.Z. Wang, X. L. Deng, Y. Li, H. K. Liu, *Electrochim. Acta*, 2009, **55**, 504.
- 23 Y. Yao, J. Zhang, T. Huang, H. Mao, A. Yu, *Int. J. Electrochem. Sci.*, 2013, **8**, 3302.
- 24 X. Yang, K. Fan, Y. Zhu, J. Shen, X. Jiang, P. Zhao, C. Li, *J. Mater. Chem.*, 2012, **22**, 17278.